NASA/TM—2002-211678

Evaluation of Mechanical Modal Characteristics Using Optical Techniques

John Lekki and Grigory Adamovsky
Glenn Research Center, Cleveland, Ohio

Patrick Flanagan
Cleveland State University, Cleveland, Ohio

Ken Weiland
Glenn Research Center, Cleveland, Ohio

June 2002

The NASA STI Program Office . . . in Profile

Since its founding, NASA has been dedicated to the advancement of aeronautics and space science. The NASA Scientific and Technical Information (STI) Program Office plays a key part in helping NASA maintain this important role.

The NASA STI Program Office is operated by Langley Research Center, the Lead Center for NASA's scientific and technical information. The NASA STI Program Office provides access to the NASA STI Database, the largest collection of aeronautical and space science STI in the world. The Program Office is also NASA's institutional mechanism for disseminating the results of its research and development activities. These results are published by NASA in the NASA STI Report Series, which includes the following report types:

- TECHNICAL PUBLICATION. Reports of completed research or a major significant phase of research that present the results of NASA programs and include extensive data or theoretical analysis. Includes compilations of significant scientific and technical data and information deemed to be of continuing reference value. NASA's counterpart of peer-reviewed formal professional papers but has less stringent limitations on manuscript length and extent of graphic presentations.

- TECHNICAL MEMORANDUM. Scientific and technical findings that are preliminary or of specialized interest, e.g., quick release reports, working papers, and bibliographies that contain minimal annotation. Does not contain extensive analysis.

- CONTRACTOR REPORT. Scientific and technical findings by NASA-sponsored contractors and grantees.

- CONFERENCE PUBLICATION. Collected papers from scientific and technical conferences, symposia, seminars, or other meetings sponsored or cosponsored by NASA.

- SPECIAL PUBLICATION. Scientific, technical, or historical information from NASA programs, projects, and missions, often concerned with subjects having substantial public interest.

- TECHNICAL TRANSLATION. English-language translations of foreign scientific and technical material pertinent to NASA's mission.

Specialized services that complement the STI Program Office's diverse offerings include creating custom thesauri, building customized data bases, organizing and publishing research results . . . even providing videos.

For more information about the NASA STI Program Office, see the following:

- Access the NASA STI Program Home Page at ***http://www.sti.nasa.gov***

- E-mail your question via the Internet to help@sti.nasa.gov

- Fax your question to the NASA Access Help Desk at 301–621–0134

- Telephone the NASA Access Help Desk at 301–621–0390

- Write to:
  NASA Access Help Desk
  NASA Center for AeroSpace Information
  7121 Standard Drive
  Hanover, MD 21076

NASA/TM—2002-211678

Evaluation of Mechanical Modal Characteristics Using Optical Techniques

John Lekki and Grigory Adamovsky
Glenn Research Center, Cleveland, Ohio

Patrick Flanagan
Cleveland State University, Cleveland, Ohio

Ken Weiland
Glenn Research Center, Cleveland, Ohio

Prepared for the
Ninth Annual International Symposium on Smart Structures and Materials
sponsored by the International Society for Optical Engineering
San Diego, California, March 17–21, 2002

National Aeronautics and
Space Administration

Glenn Research Center

June 2002

The Aerospace Propulsion and Power Program at
NASA Glenn Research Center sponsored this work.

Available from

NASA Center for Aerospace Information
7121 Standard Drive
Hanover, MD 21076

National Technical Information Service
5285 Port Royal Road
Springfield, VA 22100

Available electronically at http://gltrs.grc.nasa.gov/GLTRS

Evaluation of Mechanical Modal Characteristics Using Optical Techniques

John Lekki and Grigory Adamovsky
National Aeronautics and Space Administration
Glenn Research Center
Cleveland, Ohio 44135

Patrick Flanagan
Cleveland State University
Cleveland, Ohio

Ken Weiland
National Aeronautics and Space Administration
Glenn Research Center
Cleveland, Ohio 44135

Abstract

In this paper the sensitivity of embedded fiber optic sensors to changes in modal characteristics of plates is discussed. In order to determine the feasibility of embedded fiber Bragg gratings for the detection of modal shapes and modal frequencies, a comparison of holographically imaged modes and the detected dynamic strain from embedded fiber optic Bragg gratings is made. Time averaged optical holography is used for the detection of mechanical defects, or damage, in various aerospace components. The damage is detected by measuring an alteration in structural dynamics, which is visually apparent when using time-averaged holography. These shifts in the mode shapes, both in frequency of the resonance and spatial location of vibration nodes, are caused by changes in parameters that affect the structure's mechanical impedance, such as stiffness, mass and damping, resulting from cracks or holes. It is anticipated that embedded fiber optic sensor arrays may also be able to detect component damage by sensing these changes in modal characteristics. This work is designed to give an initial indication to the feasibility of damage detection through the monitoring of modal frequencies and mode shapes with fiber optic sensors.

1. Introduction

Damage or structural defects in an aerospace component can affect the resonant modal characteristics of that component. These defects have been detected using time-averaged holography[1] where they show up as changes in the mode shape when the component is vibrated at a resonant frequency or as a shift in the value of the resonant frequency. At the NASA, John H. Glenn Research Center, time-averaged holography has been used to detect cracks in turbine blades and for the inspection of cold plates for the International Space Station[2, 3]. It is anticipated that a matrix of fiber optic sensors may also be able to detect these slight changes in mode shape. As a first step in understanding the applicability of fiber optic Bragg gratings (FOBG) for this use, the sensitivity of embedded fiber Bragg gratings to modal characteristics has been examined. Both the modal frequencies and modal shapes of vibrational resonant modes have been studied. From the time-averaged holograms it is possible to visually determine if the known locations of the sensors are in or near vibrational nodes or antinodes. Using this information the magnitude of response from the Bragg grating has been correlated to whether the grating is on a node, antinode or somewhere in between. It is anticipated that given enough sensors, this relative magnitude of response will be enough information to determine the mode shape.

In this paper, results showing the correlation between holographic mode shapes and fiber sensor outputs will be presented. Results are given for two plates that have very different mechanical characteristics. The first plate tested is made from a Polymer Matrix Composite (PMC) that is very rigid, lightweight, and is also highly damping. The second plate examined is a thin copper plate that is not as rigid or lightweight as the polymer matrix composite but does have lower damping. These two materials represent two very different constituents of the spectrum of aerospace materials.

2. Experimental Setup

The sensitivity of the fiber Bragg gratings to changes in resonant mode shapes was determined by vibrating panels with embedded fiber optic Bragg gratings at resonant frequencies and examining the return signals from the attached / embedded fiber sensors. As previously mentioned there were two different plates tested. The first plate tested is made of PMC and has a single fiber Bragg grating sensor embedded within. The second plate tested is made of copper and has three Bragg gratings glued (with epoxy) into a grove machined in the panel. Both panels are the same length and width, 102 mm × 152 mm respectively. The PMC plate has a thickness of 2.86 mm and the copper plate has a thickness of 0.813 mm.

The experimental setup for studying the response of the fiber sensors embedded into the polymer matrix composite plate is shown schematically in figure 1. In order to isolate the signal processing system for the sensors from the acoustic system that was used to vibrate the plate, the demodulation system was located in a separate room about 20 meters away and fibers to connect the system to the sensors

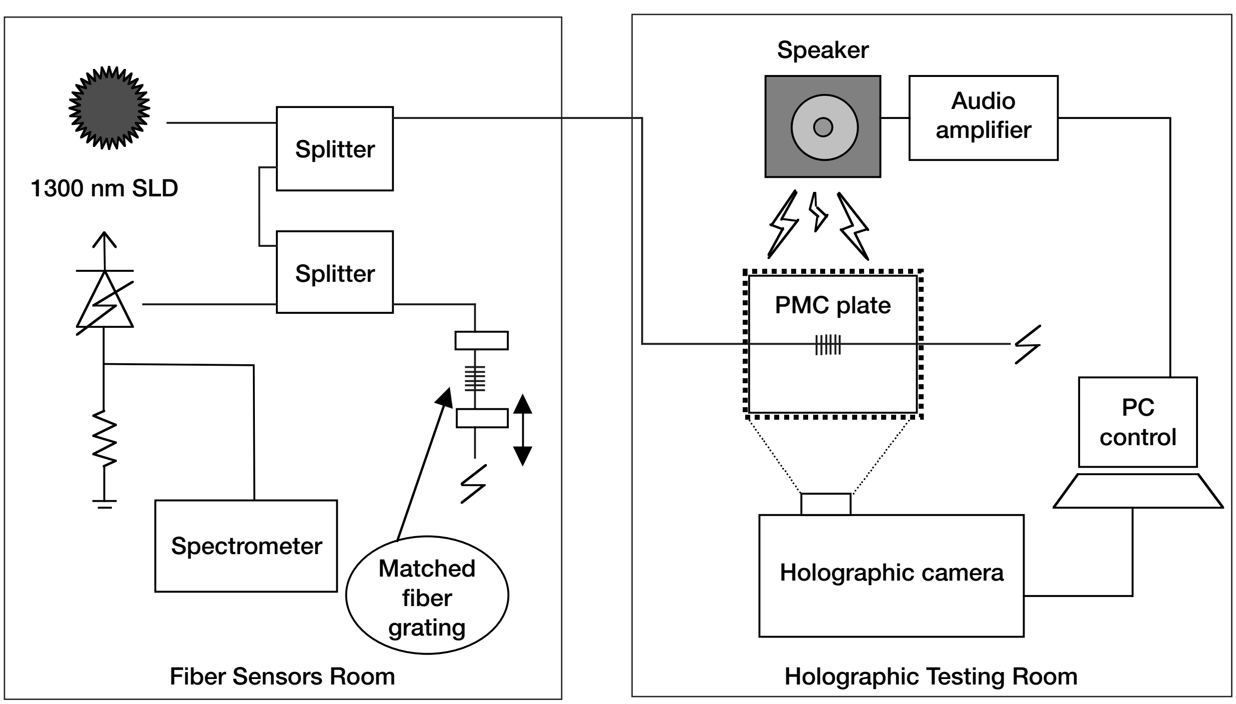

Figure 1.—Diagram of test configuration for polymer matrix composite plate.

were run between the rooms. In the Holographic Testing room an existing system[2] was used to vibrate the plate and acquire time averaged holograms of the plate. This system consisted of a commercially available holocamera and a speaker driven by an audio amplifier. The PMC plate was mounted in a holder so that all four edges were fixed. This holder is similar to the one used for the copper plate that is shown in figure 2 except that the copper plate is fixed on only two edges. The laser used to make the holograms is a diode pumped Nd:YAG laser that is doubled internally to a wavelength of 532 nm. In order to make holograms of the resonant modes, an oscillator in the computer drives the speaker at one of the resonant frequencies of the plate. The speaker is placed directly behind the plate and the amplifier output amplitude is increased until the plate begins to resonate. The holographic images are acquired and processed using the holocamera system. The technique is called time averaged holography because the image is acquired over 1/60 of a second during which time there are one or more vibration cycles. The holocamera system produces an image with an intensity pattern at a given point on the surface proportional to

$$I \propto J_0^2\,(2\pi K \bullet \delta),$$

where I is the intensity, J_0 is the zero order Bessel function, δ is the amplitude of vibration displacement vector expressed in terms of multiples of the wavelength of the laser light (532 nm) and K is the sensitivity vector[2]. So in this configuration, where the holographic images are taken at normal incidence to the vibrating plate, each fringe, light and dark pair, represents one wavelength of displacement normal to the image plane. In this case the fringes can be thought of as contour lines of constant displacement.

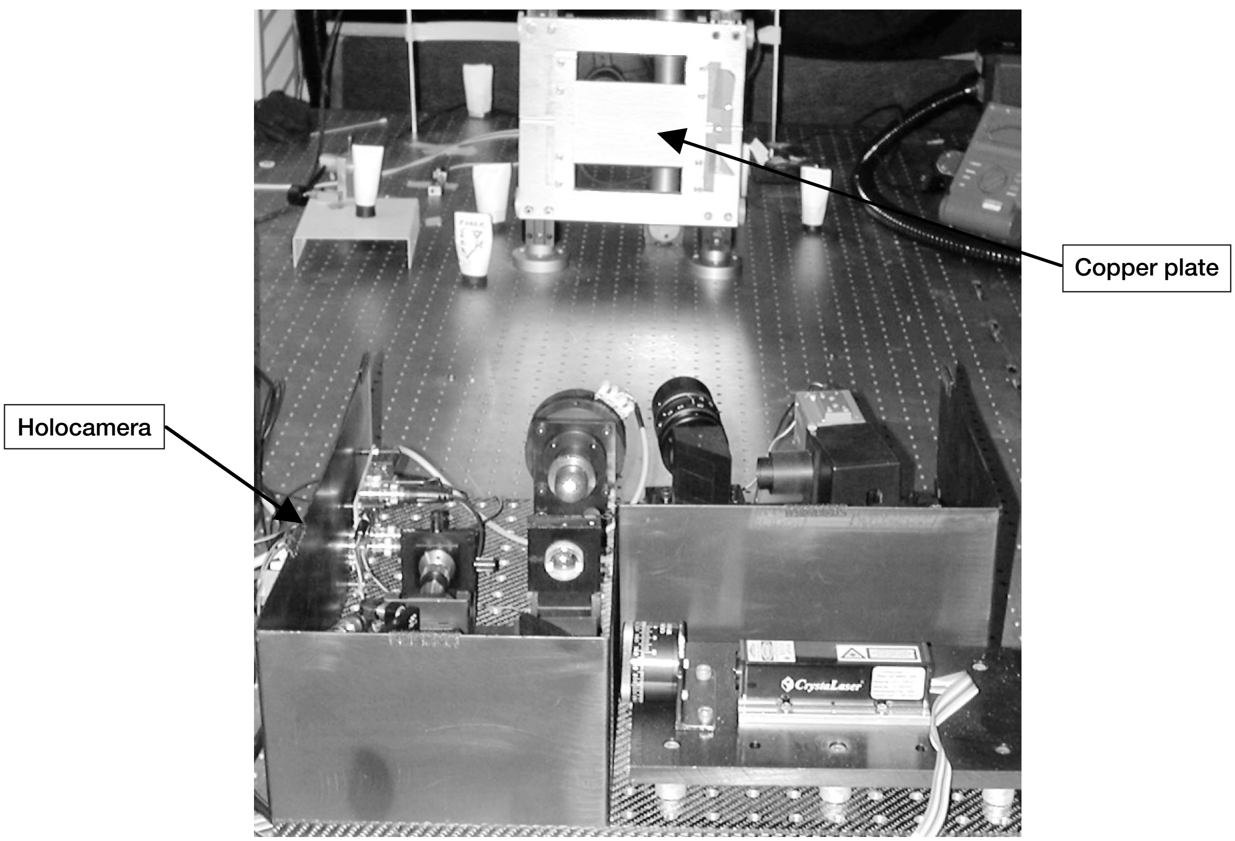

Figure 2.—Picture of the experimental setup for holographic imaging. The holographic camera is in the foreground and copper plate is shown inside the test fixture located at the top of the picture. The speaker used to vibrate the plate is directly behind the copper plate.

The fiber optic system consists of a 1300 nm super luminescent diode light source, a 1300 nm high temperature Bragg grating sensor in the PMC plate, a matched reference Bragg grating used for wavelength demodulation[4], a high frequency photodiode and a spectrometer for power spectrum measurement. There is only a single sensor in the plate used here because it was originally instrumented for measuring the internal temperatures of the PMC plate during the manufacturing process and was made before this work began[5]. The fiber Bragg grating sensor is located in the center of the panel and the fiber runs parallel to the long axis of the panel (the long axis goes from left to right in the holographic images).

Using a matched fiber Bragg grating for wavelength demodulation provides the high degree of stability and sensitivity required for this experiment. The system is configured so that the matched grating reflects a portion of the filtered light back through the splitter to the photodiode. The matched grating is set to reflect a particular wavelength by straining the grating between a fixed holder and a holder that is translated using a micrometer. Each day of the experiment the matched grating was set at a wavelength that produced the highest change in reflected light power for a given shift in the sensor's wavelength. As the sensor in the plate is dynamically strained the center wavelength of the reflected light will shift. This shift in wavelength changes the amount of power that is reflected from the matched grating and measured with the photodiode. Thus the wavelength shift in the reflected light from the sensor results in a change in voltage from the photodiode.

The experimental setup for the copper plate is very similar to that of the PMC plate and is shown in figure 3. For the copper plate three fibers were attached to the plate. The plate was mounted into the fixture with only the two short edges fixed and the configuration of the demodulation system was changed slightly. The three fibers were glued into a groove in the plate that was machined to a depth of 0.2 mm. The groove runs parallel to the long axis of the plate and is centered in the short dimension of the plate. The Bragg gratings in the copper plate will from here on be designated as sensor # (1, 2, or 3). The centers of sensors 1, 2 and 3 are located a distance of 38 mm, 76 mm and 114 mm respectively from the left edge of the plate. The demodulation system was changed so that the matched grating acted like a filter

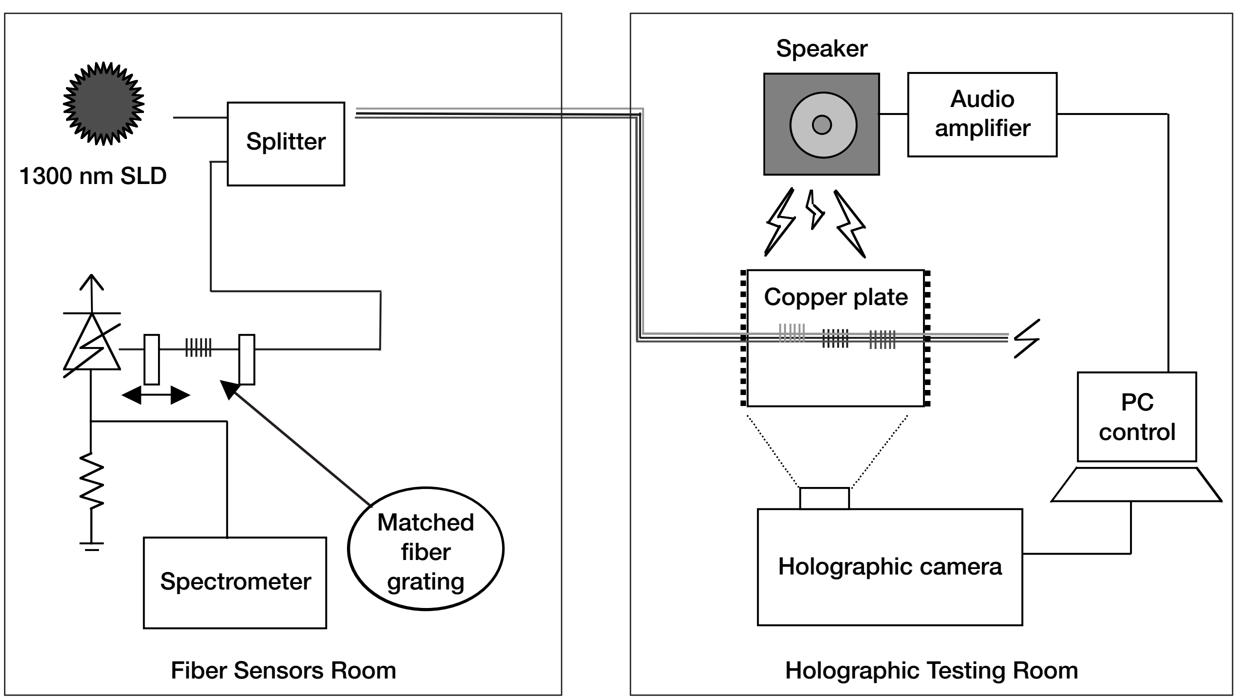

Figure 3.—Diagram of test configuration for the copper plate.

and the photodiode received the light that was passed through. This produced the same result as the configuration for the PMC sensor but did decrease the complexity of the system because one less splitter was required. In testing the copper plate, each sensor was monitored individually so that a single light source and single demodulation system could be used for all three sensors. This kept the noise introduced from the light source and the sensitivity of the demodulation system equivalent for each sensor. Changing the sensor that was monitored was accomplished by disconnecting one sensor from the demodulation system and connecting another.

3. Experimental Results and Analysis

The objective of this experiment was to determine the capability of FOBG sensors to detect resonant mode characteristics. The two characteristics that FOBGs have been found to detect, through correlation with time-averaged holograms, are the resonant frequency for a particular mode and the relative strain at different locations within the mode shape. The experimental analysis supporting these conclusions is presented further here.

The initial tests performed with the PMC plate were to demonstrate the range of resonant frequencies that can be detected using the fiber optic sensor and the ability of the sensor to determine the modal frequency. The signal from the sensor had a very high signal to noise ratio at all modal frequencies tested, up to about 4 KHz. This upper value is not a limit, but is the maximum frequency at which we chose to vibrate the plate. Figure 4(a) is a hologram of the resonant mode at 706 Hz. From the holographic image the amount of displacement at a given antinode can be determined by counting the number of fringes from the node to the peak of the antinode and than multiplying that number by the wavelength of the laser light (532 nm). For this particular mode the displacement at the center of the antinode is 5.8 microns and the signal from the fiber sensor measured 64 pV^2 rms on the spectrometer. This signal level is well above the noise floor of approximately 10 pV^2 rms. In contrast however the resonant mode at a frequency of 3.062 KHz, shown in figure 4(b), has a much lower displacement at the center, 1.8 microns, but produces a stronger signal from the FOBG, 96 pV^2 rms. This implies that the sensor may be more sensitive to mode shapes at higher frequencies because the fiber optic sensor appears to be sensitive to the spatial frequency of the nodes and antinodes, which is higher at higher acoustic frequencies. As the distance between the nodes and antinodes decreases, as will happen for modes that have higher resonant frequency, the radius

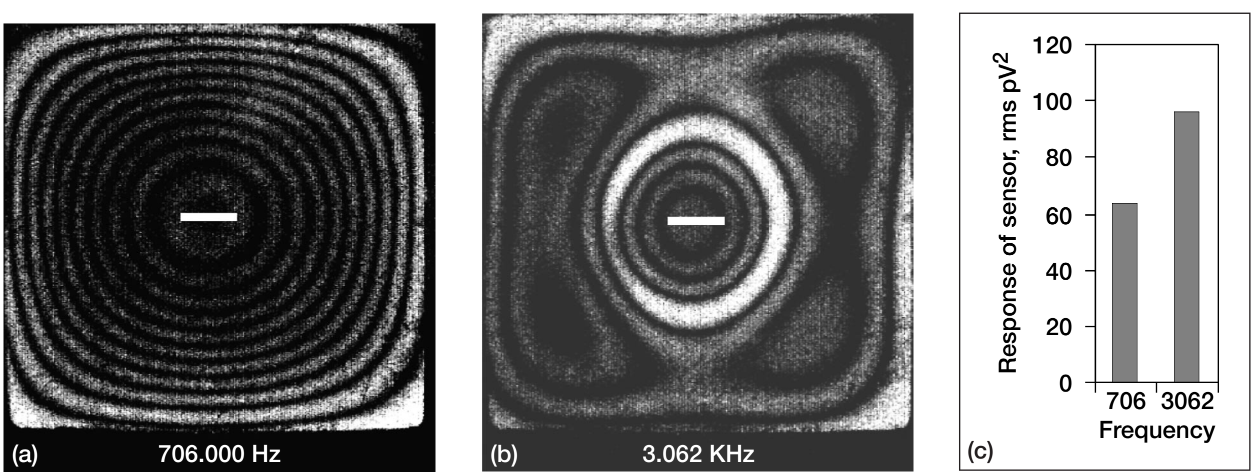

Figure 4.—(a) Holographic image of the 706 Hz resonant mode of the PMC plate. (b) Holographic image of the 3.062 KHz resonant mode of the PMC plate. (c) Graph comparing the response of the embedded fiber sensor for two resonant frequencies.

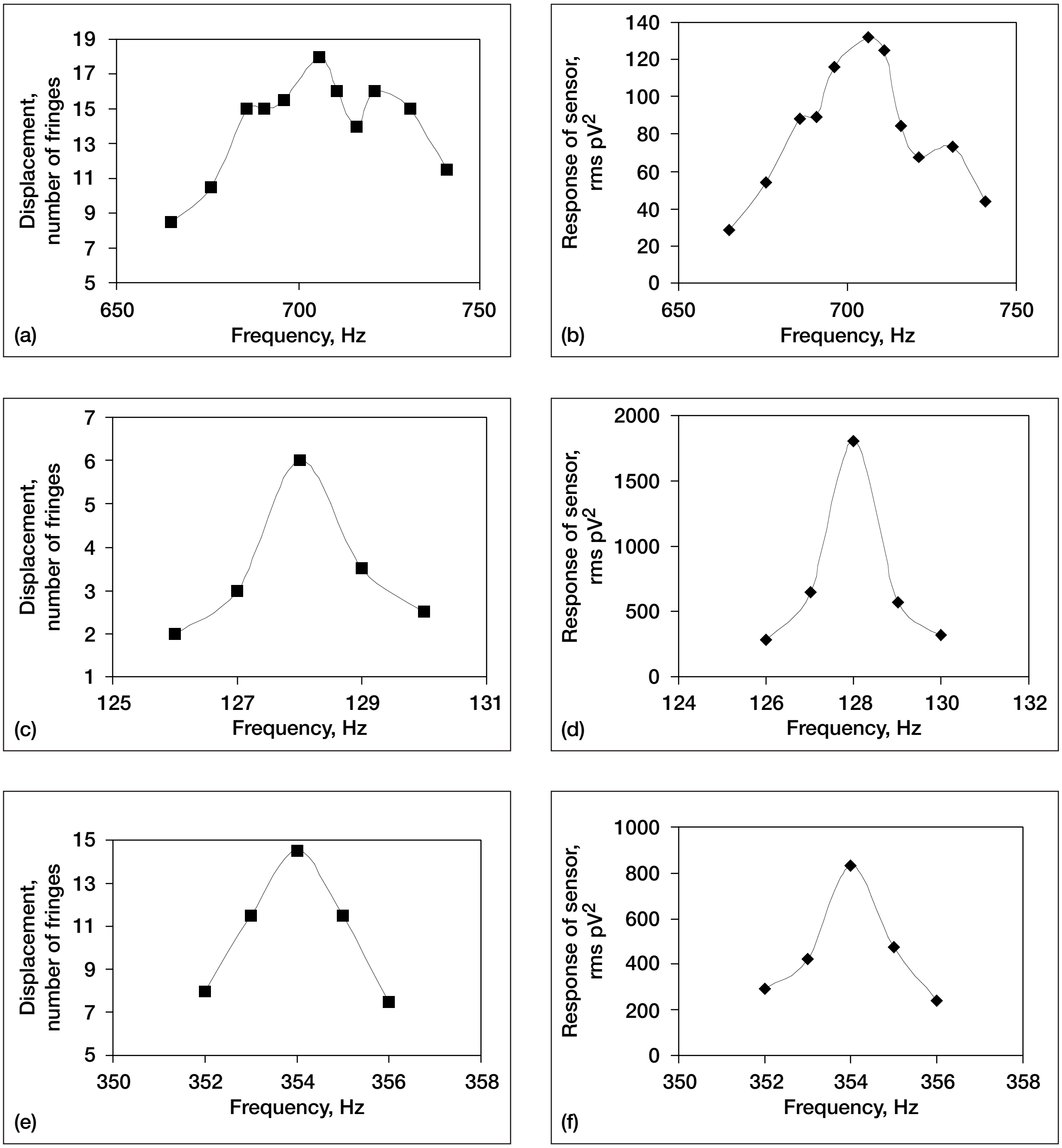

Figure 5.—(a) Fringe displacement as a function of frequency for the first resonant mode of the PMC plate. (b) Sensor response of embedded sensor as a function of frequency for the first resonant mode of the PMC plate. (c) Fringe displacement as a function of frequency for the first resonant mode of the copper plate. (d) Response of sensor 2 as a function of frequency for the first resonant mode of the copper plate. (e) Fringe displacement as a function of frequency for the third resonant mode of the copper plate. (f) Response of sensor 3 as a function of frequency for the third resonant mode of the copper plate.

of curvature for the plate at the antinodes will decrease causing the strain to increase for a given displacement. This fact adds to the feasibility of using the FOBG sensors at higher frequencies.

The results from the PMC plate showed that the fiber sensor can be used to properly identify the resonant frequency. Here the resonant frequency for a mode is defined as the frequency that produces the greatest displacement at the center of the antinodes given a constant forcing function. The identification of the resonant frequency using fiber sensors is illustrated by comparing the number of fringes in the hologram to the dynamic signal from the FOBG sensor for several frequencies at or near resonance. The number of fringes in the hologram as a function of the vibrating frequency is graphed in figure 5(a). At the same time the response of the sensor was measured at these frequencies and a plot of these values is shown in figure 5(b). These two graphs both show that the resonant frequency is 706 Hz. This test was also done with two resonant modes (modes 1 and 3) of the copper plate. In both of these cases the resonant frequency, as determined by the fiber optic sensor and through holography, matched exactly. The data concerning these two modes are shown in figure 5(c-f).

The sensitivity of the fiber optic sensors to detecting the relative dynamic strain in different locations for a particular mode was investigated using the copper plate because of its multiple sensors. For the first resonant mode the hologram is shown in figure 6(a) and the output of the three sensors is graphed in figure 7(a). The center sensor has the highest output and the two sensors on either side have a much lower output. The symmetry of these readings agree with the symmetry of the holographic fringes for this mode. As shown in figure 8(a), these readings also agree with the inverse relationship of the radius of curvature, R, and strain, ε,

$$\varepsilon \propto \frac{1}{R}.$$

Sensors 1 and 3 are in relatively flat areas of the curve and so should have small strain and sensor 2 has the smallest radius of curvature and hence the largest dynamic strain.

The third resonant mode, shown in figure 6(b), is good for drawing comparisons of the relative response of the sensors because it contrasts nicely with the first resonant mode. In the first resonant mode sensor 2 is in the middle of the antinode of the vibration. In the third resonant mode sensor 2 is instead located at a node. This sensor now is in a relatively flat location, as shown in figure 8(b), and is no longer

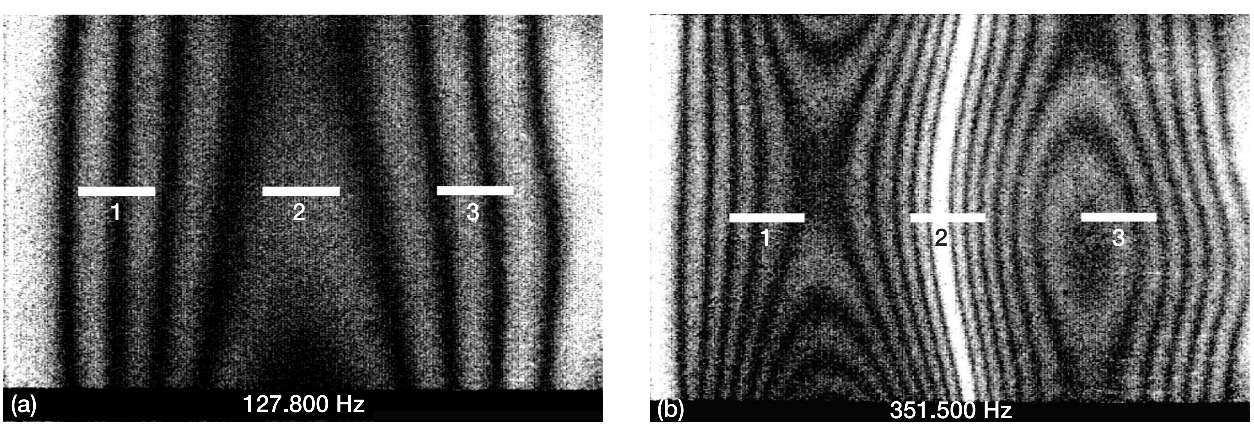

Figure 6.—(a) Holographic images of (a) first and (b) third resonant modes. The locations of the sensors are shown as white lines on the images. In each image, sensor 1 is located on the left, sensor 2 in the middle and sensor 3 on the right.

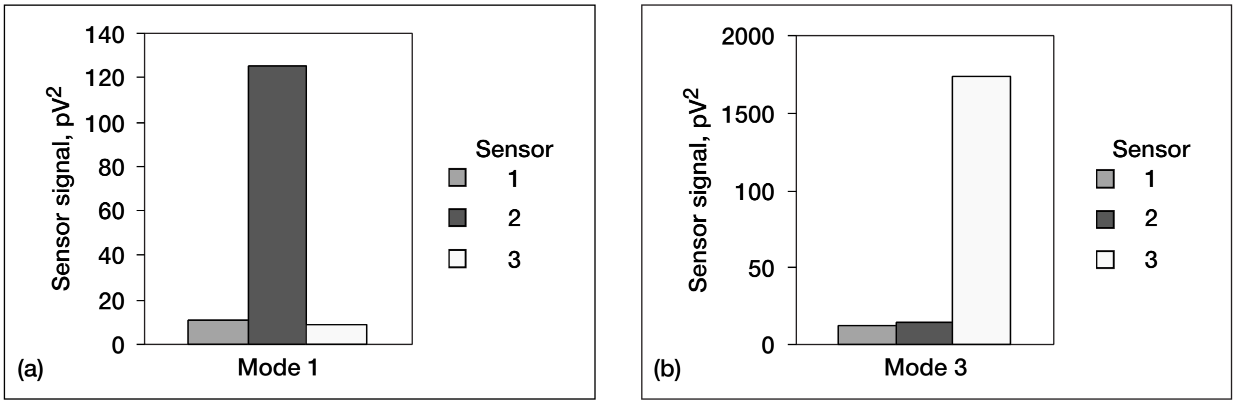

Figure 7.—The dynamic response of fiber Bragg gratings in the copper plate for the (a) first and (b) third resonant modes.

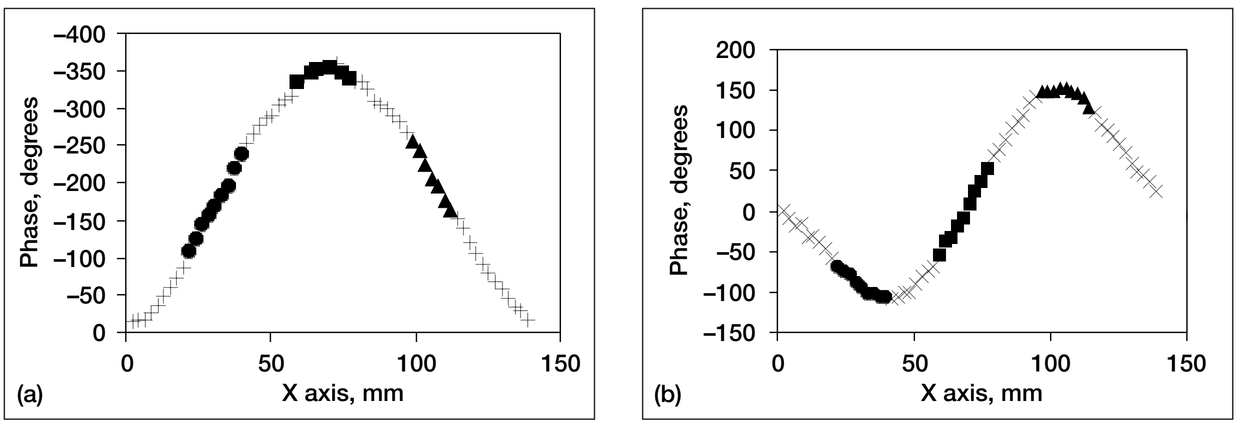

Figure 8.—Phase maps generated from the holographic images by the holocamera software for (a) Mode 1 and (b) Mode 3. Circles, squares and triangles denote the points corresponding to sensors 1, 2 and 3 respectively.

experiencing the largest amount of strain, as shown in figure 7(b). This change of location of nodes and antinodes is also significant for sensors 1 and 3. In the first resonant mode they are in a location that is halfway between the anti node and the node and is relatively flat. This changes in the third resonant mode where they are now located at the anti nodes where there is significant curvature. These two sensors have a very large increase in dynamic response, a factor of 10 for sensor 1 and a factor of 190 for sensor 3. Sensor 3 has by far the largest output. This asymmetry was not expected as it was assumed that both sensors 1 and 3 would have similar outputs if the third mode were perfectly symmetrical. However the hologram of this mode, shown in figure7(b), confirms the asymmetry of the mode. If the mode were perfect the bright fringe in the middle of the hologram would be straight instead of curved and the two circular anti nodes would be mirror images of one another. The phase map in figure 8b also shows that sensor 1 is off of the curved portion of the mode while sensor 3 is right on it. The differences in curvature for the two sensors and the greater displacement for sensor 3 relative to sensor 1 appear to explain the asymmetry of the sensor outputs. This asymmetrical mode has serendipitously provided evidence that the embedded sensors are sensitive to imperfections in the mode shape, as may be caused by damage. This agreement of the holographic images with the sensor data has led us to believe that an array of fiber sensors should be able to accurately characterize a resonant mode just as is presently done using time averaged holography.

4. Summary

Fiber optic Bragg sensors have been shown to be able to closely reflect simple mode shapes of plates and detect the resonant frequencies of these modes. This has been confirmed by taking dynamic data from fiber optic sensors embedded in or attached to plates while acquiring time-averaged holograms of the vibrating plates. The two plates have significantly different material characteristics so it can be presumed that these conclusions would be true for many other materials. Further testing should be continued with an array of many more sensors to verify these conclusions for higher frequency modes. These results, which show that modal characteristics are detectable through in-situ fiber optic sensors, indicate that future research into the sensitivity of these sensors to changes in mode characteristics caused by component damage is warranted.

5. References

1. S. W. Doebling, C. R. Farrar and M. B. Prime, "A Summary Review of Vibration-Based Damage Identification Methods", The Shock and Vibration Digest, 30, pp. 91–105, 1998.
2. A. J. Decker, M. E. Melis and K. E. Weiland, "Inspection of Space Station Cold Plate Using Visual and Automated Holographic Techniques", NASA/TM—1999-209388, Aug. 1999.
3. A. J. Decker, "Optimization of Training Sets for Neural-Net Processing of Characteristic Patterns From Vibrating Solids", NASA/TM—2001-210979, July 2001.
4. I. Perez, H. Cui and E. Udd, "Acoustic Emission Detection Using Fiber Bragg Gratings", Proceedings of SPIE, Vol. 4328, pp. 209–215, 2001.
5. G. Adamovsky, J. Lekki, J. K. Sutter, S.S. Sarkisov, M. J. Curley and C. E. Martin, "Smart Microsystems with photonic element and their applications to aerospace platforms", NASA/TM—2000-210607, December 2000.

REPORT DOCUMENTATION PAGE

Form Approved
OMB No. 0704-0188

1. AGENCY USE ONLY (*Leave blank*)	2. REPORT DATE	3. REPORT TYPE AND DATES COVERED
	June 2002	Technical Memorandum

4. TITLE AND SUBTITLE

Evaluation of Mechanical Modal Characteristics Using Optical Techniques

5. FUNDING NUMBERS

WU–708–87–13–00

6. AUTHOR(S)

John Lekki, Grigory Adamovsky, Patrick Flanagan, and Ken Weiland

7. PERFORMING ORGANIZATION NAME(S) AND ADDRESS(ES)

National Aeronautics and Space Administration
John H. Glenn Research Center at Lewis Field
Cleveland, Ohio 44135–3191

8. PERFORMING ORGANIZATION REPORT NUMBER

E–13395

9. SPONSORING/MONITORING AGENCY NAME(S) AND ADDRESS(ES)

National Aeronautics and Space Administration
Washington, DC 20546–0001

10. SPONSORING/MONITORING AGENCY REPORT NUMBER

NASA TM—2002-211678

11. SUPPLEMENTARY NOTES

Prepared for the Ninth Annual International Symposium on Smart Structures and Materials sponsored by the International Society for Optical Engineering, San Diego, California, March 17–21, 2002. John Lekki, Grigory Adamovsky, and Ken Weiland, NASA Glenn Research Center; Patrick Flanagan, Cleveland State University, Department of Mechanical Engineering, Cleveland, Ohio. Responsible person, John Lekki, organization code 5520, 216–433–5650.

12a. DISTRIBUTION/AVAILABILITY STATEMENT

Unclassified - Unlimited
Subject Category: 74 Distribution: Nonstandard

Available electronically at http://gltrs.grc.nasa.gov/GLTRS

This publication is available from the NASA Center for AeroSpace Information, 301–621–0390.

12b. DISTRIBUTION CODE

13. ABSTRACT ***(Maximum 200 words)***

In this paper the sensitivity of embedded fiber optic sensors to changes in modal characteristics of plates is discussed. In order to determine the feasibility of embedded fiber Bragg gratings for the detection of modal shapes and modal frequencies, a comparison of holographically imaged modes and the detected dynamic strain from embedded fiber optic Bragg gratings is made. Time averaged optical holography is used for the detection of mechanical defects, or damage, in various aerospace components. The damage is detected by measuring an alteration in structural dynamics, which is visually apparent when using time-averaged holography. These shifts in the mode shapes, both in frequency of the resonance and spatial location of vibration nodes, are caused by changes in parameters that affect the structure's mechanical impedance, such as stiffness, mass and damping, resulting from cracks or holes. It is anticipated that embedded fiber optic sensor arrays may also be able to detect component damage by sensing these changes in modal characteristics. This work is designed to give an initial indication to the feasibility of damage detection through the monitoring of modal frequencies and mode shapes with fiber optic sensors.

14. SUBJECT TERMS

Fiber optics; Sensors; Holography; Modal analysis; Damage detection

15. NUMBER OF PAGES

15

16. PRICE CODE

17. SECURITY CLASSIFICATION OF REPORT	18. SECURITY CLASSIFICATION OF THIS PAGE	19. SECURITY CLASSIFICATION OF ABSTRACT	20. LIMITATION OF ABSTRACT
Unclassified	Unclassified	Unclassified	